Novel Zn(II), Co(II) and Cu(II) diflunisalato complexes with neocuproine and their exceptional antiproliferative activity against cancer cell lines

Romana Smolková,*[a] Lukáš Smolko,[b] Erika Samoľová,[c] Ibrahim Morgan,[d] Robert Rennert [d] and Goran N. Kaluđerović [e]

Electronic Supplementary Information (ESI)

Table of Contents

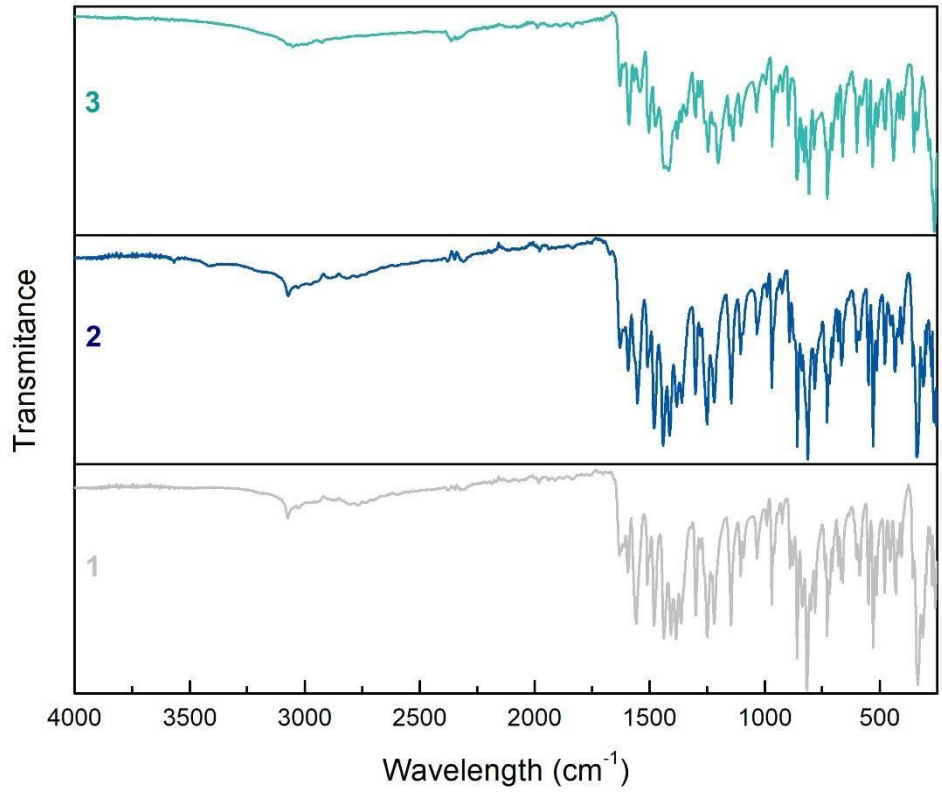

Fig. S1 Comparison of solid-state FT-IR ATR spectra of **1**, **2** and **3**.

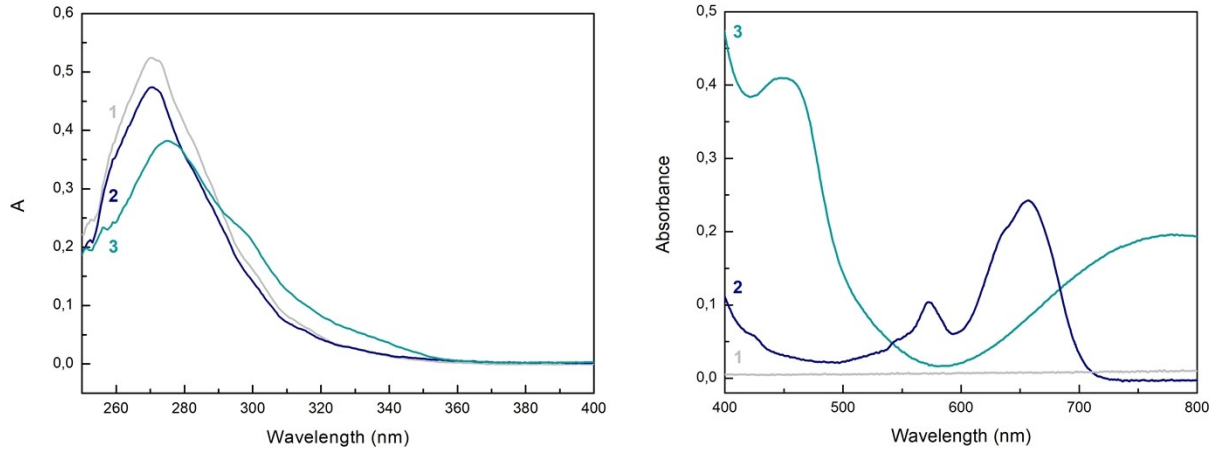

Fig. S2 Absorption spectra of DMSO solutions of **1**, **2** and **3** in the UV (left, 10 µM) and visible region (right, 1000 µM).

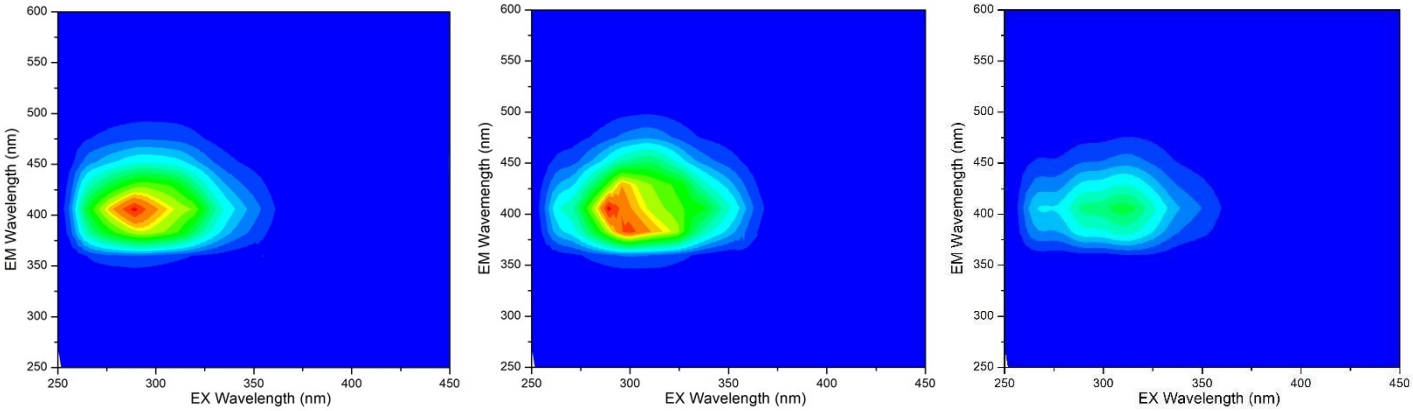

Fig. S3 Excitation-emission matrices (EEMs) of complex **1** (left), **2** (middle) and **3** (right) in 10 µM DMSO solutions adjusted to the same intensity colour scale for better comparison (Rayleigh and Raman scattering is masked).

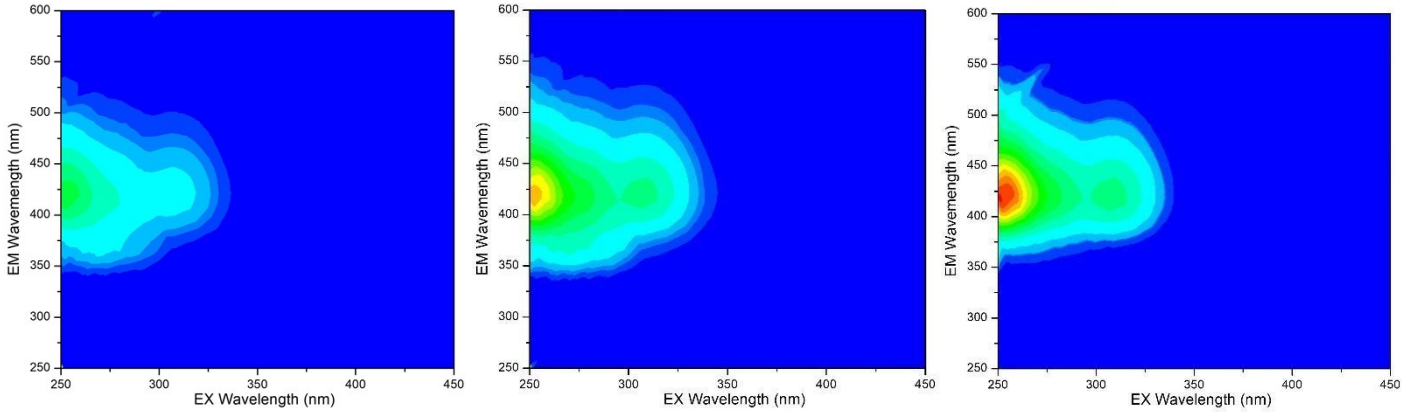

Fig. S4 Excitation-emission matrices (EEMs) of complex **1** (left), **2** (middle) and **3** (right) in 10 µM aqueous solutions adjusted to the same intensity colour scale for better comparison (Rayleigh and Raman scattering is masked).

Table S1 Crystal data and structure refinement for complexes **1**, **2** and **3**.

Compound	**1**	**2**	**3**
CCDC reference number	**2345890**	**2345891**	**2345892**
Empirical formula	$C_{27}H_{19}N_2O_3F_2Cl_1Zn_1$	$C_{27}H_{19}N_2O_3F_2Cl_1Co_1$	$C_{27}H_{18}N_2O_3F_2Cl_1Cu_1$
Formula weight	558.3	551.8	555.4
Temperature [K]	120	120	120
Wavelength [Å]	1.54184	1.54184	1.54184
Crystal System	monoclinic	monoclinic	triclinic
Space Group	$P2_1/n$	$P2_1/n$	P-1
a [Å]	11.5013(1)	11.6277(7)	9.4922(3)
b [Å]	12.6985(1)	12.6340(5)	9.7102(3)
c [Å]	15.3433(1)	15.2269(7)	13.8187(4)
α [°]	90	90	90.538(3)
β [°]	95.733(1)	95.864(4)	97.661(2)
γ [°]	90	90	115.412(3)
Volume [Å^3]	2229.67(3)	2225.19(19)	1137.02(7)
Z	4	4	2
ρ(calculated) [g.cm^{-3}]	1.6631	1.6472	1.6224
μ [mm^{-1}]	3.09	0.944	2.885
F000	1136	1124	567
Crystal colour and shape	colourless needle	blue prism	brown prism
Crystal dimensions [mm]	0.32 × 0.18 × 0.17	0.12 × 0.10 × 0.08	0.21 × 0.17 × 0.10
ϑ range for data collection [°]	4.53 – 67.54	3.14 – 28.59	3.24 – 67.36
Reflections collected	48200	29802	24668
Independent reflections	4023	5344	4077
R_{int}	0.0326	0.0400	0.0521
Data/restraints/parameters	4023/0/329	5344/0/329	4077/0/339
Goodness-of-fit*	2.79	1.77	1.94
Final R indices ($I > 3\sigma(I)$)	$R1$ = 0.0312 $wR2$ = 0.0848	$R1$ = 0.0368 $wR2$ = 0.0785	$R1$ = 0.0380 $wR2$ = 0.0874
R indices (all data)	$R1$ = 0.0329 $wR2$ = 0.0853	$R1$ = 0.0527 $wR2$ = 0.0818	$R1$ = 0.0433 $wR2$ = 0.0896
Max. and min. residual electron density [e. Å^{-3}]	0.63; -0.66	0.93; -0.53	0.91; -0.41

* The program JANA does not refine the weighting scheme to reach Goodness of fit close to 1. The displayed GOF corresponds to the experimental weighting scheme with the instability factor as an instrumental parameter.

Table S2 Selected bond lengths and angles (A, °) for **1**, **2** and **3**.

Complex	**1** (M = Zn)	**2** (M = Co)	**3** (M = Cu)
M1-O1	1.962(1)	1.977(1)	1.963(2)
M1-O2	2.873(2)*	2.660(2)*	2.308(2)
M1-N1	2.051(2)	2.038(2)	1.993(2)
M1-N2	2.082(2)	2.075(2)	2.039(2)
M1-Cl1	2.193(1)	2.221(1)	2.313(1)
O1-M1-O2	-	-	60.94(7)
N1-M1-N2	81.60(7)	81.83(7)	82.97(8)
O1-M1-N1	106.05(6)	109.27(6)	152.62(8)
O1-M1-N2	128.21(6)	135.16(6)	98.66(8)
O2-M1-N1	-	-	100.15(8)
O2-M1-N2	-	-	138.97(7)
Cl1-M1-O1	105.02(4)	101.18(4)	96.28(6)
Cl1-M1-O2	-	-	97.36(5)
Cl1-M1-N1	119.77(5)	116.63(5)	106.26(6)
Cl1-M1-N2	115.10(5)	112.36(5)	121.26(6)

* M1-O2 distance is too long to be considered as a standard coordination bond

Table S3 Possible hydrogen bonding interactions (A, °) for **1** and **2**.

D–H···A	**d(D–H)**	**d(H···A)**	**d(D···A)**	**<(DHA)**
1				
O3-H1O3···O2	0.82(4)	1.81(3)	2.565(2)	153(3)
C10-H1C10···O2^{i}	0.96	2.26	3.175(3)	159
C4-H1C4···Cl1^{ii}	0.96	2.69	3.455(2)	137
C16-H1C16···Cl1^{iii}	0.96	2.75	3.653(2)	157
2				
O3-H1O3···O2	0.76(2)	1.91(2)	2.594(2)	150(2)
C10-H1C10···O2^{i}	0.96	2.30	3.215(3)	160
C4-H1C4···Cl1^{ii}	0.96	2.68	3.463(2)	139
C16-H1C16···Cl1^{iii}	0.96	2.76	3.658(2)	157

Symmetry code: (i) ½+x, ½-y, ½+z; (ii) ½+x, ½-y, -½+z; (iii) -½+x, ½-y, -½+z

Table S4 Selected π-π interactions (A, °) for **1** and **2**.

Cg(I)···Cg(J)	d(Cg···Cg)	α	β	γ
1				
Cg3···Cg2^{i}	3.809(1)	5.48(10)	28.6	25.4
Cg2···Cg1^{iv}	3.892(1)	8.11(10)	20.6	28.7
2				
Cg3···Cg2^{i}	3.794(1)	5.77(10)	24.1	27.9
Cg2···Cg1^{iv}	3.885(1)	8.54(10)	19.9	28.4

Symmetry code: (i) ½+x, ½-y, ½+z; (iv) -x, 1-y, 1-z

Aromatic rings centres of gravity: Cg1 (N1-C14-C15-C16-C17-C25); Cg2 (N2-C23-C22-C21-C20-C24); Cg3 (C8-C9-C10-C11-C12-C13)

Table S5 Possible hydrogen bonding interactions (A, °) for **3**.

D–H···A	d(D–H)	d(H···A)	d(D···A)	<(DHA)
3				
O3-H1O3···O2	0.77(5)	1.96(5)	2.628(3)	146(5)
O3-H1O3···O3^{v}	0.77(5)	2.40(5)	2.778(3)	112(5)
C21-H1C21···Cl^{vi}	0.96	2.86	3.615(3)	136
C19-H1C19···Cl^{iv}	0.96	2.83	3.592(3)	137

Symmetry code: (iv) -x, 1-y, 1-z; (v) -x, -y, -z; (vi) x, -1+y, z

Table S6 Selected π-π interactions (A, °) for **3**.

Cg(I)···Cg(J)	d(Cg···Cg)	α	β	γ
3				
Cg2···Cg1^{iv}	3.485(2)	1.69(11)	11.7	10.3
Cg3···Cg2^{vii}	3.642(1)	9.13(12)	22.6	18.9

Symmetry code: (iv) -x, 1-y, 1-z; (vii) 1+x, y, z

Aromatic rings centres of gravity: Cg1 (C17-C18-C19-C20-C24-C25); Cg2 (N2-C23-C22-C21-C20-C24); Cg3 (C8-C9-C10-C11-C12-C13)

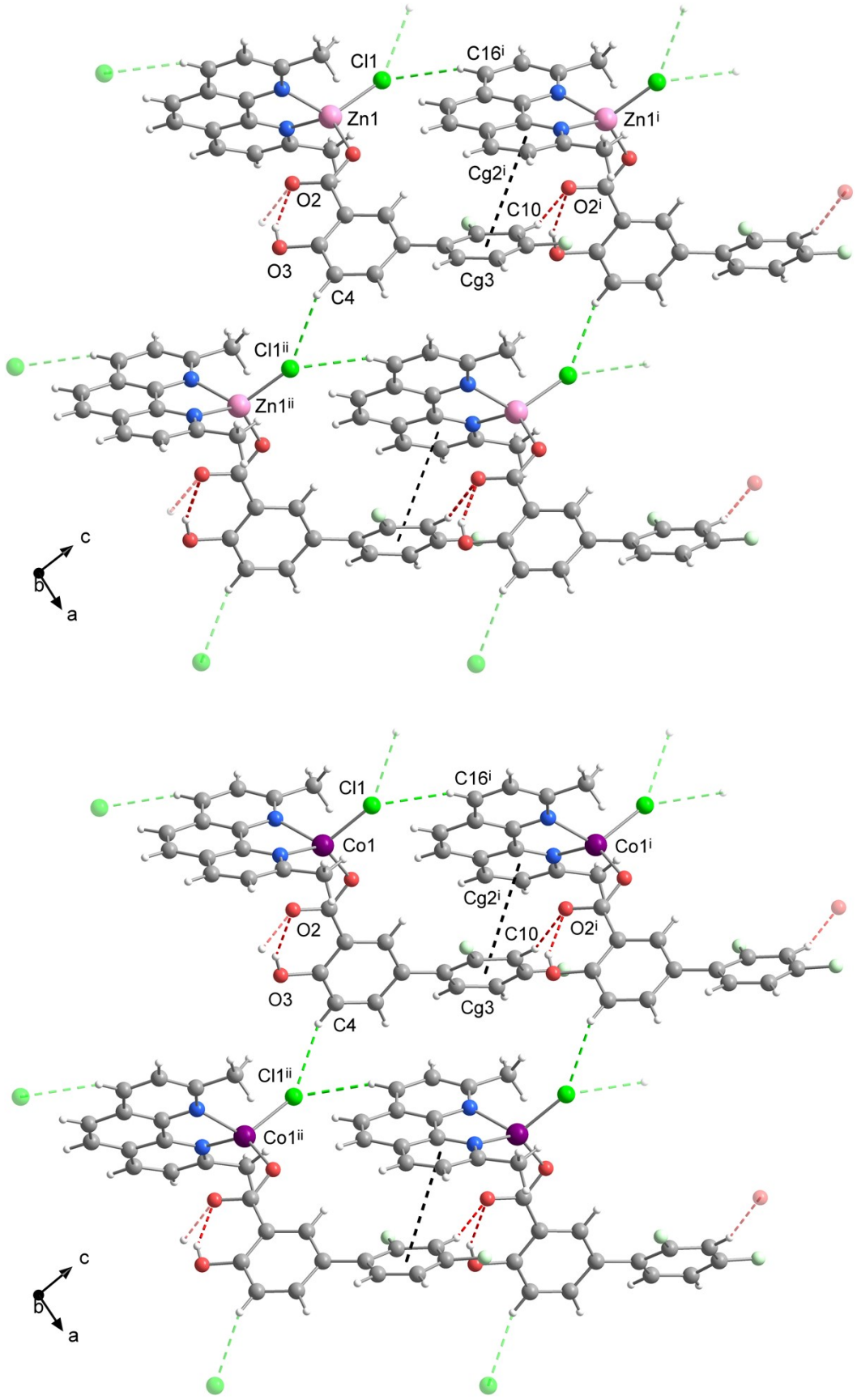

Fig. S5 Crystal packing of **1** (top) and **2** (bottom) showing intermolecular interactions linking complex molecules into supramolecular planes parallel to *ac*. Black dashed lines represent π-π stacking interactions, red and green dashed lines represent O-H···O, C-H···O and C-H···Cl hydrogen bonding interactions, respectively. Symmetry codes: (i) ½+x, ½-y, ½+z; (ii) ½+x, ½-y, -½+z.

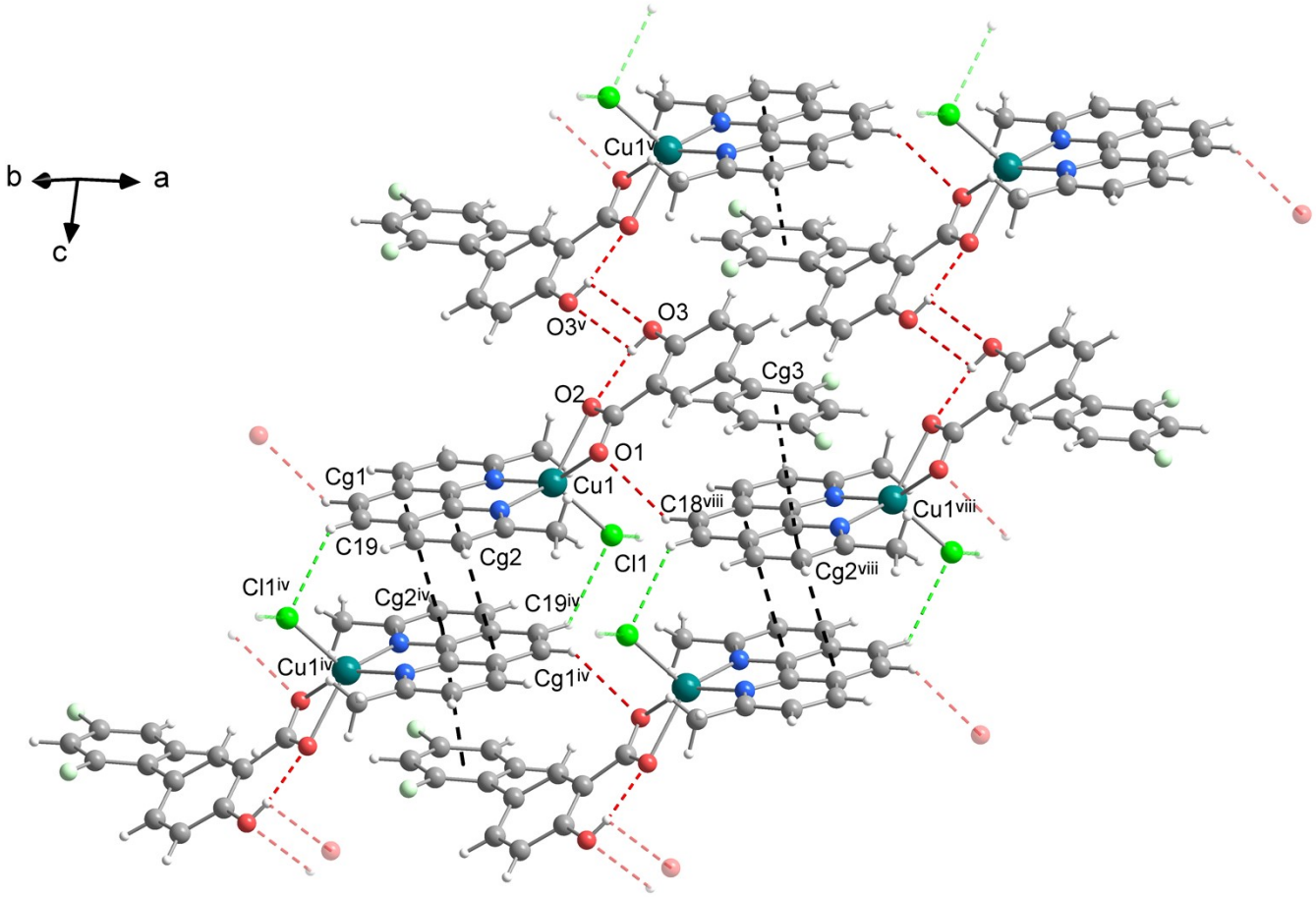

Fig. S6 Crystal packing of **3** showing intermolecular interactions linking complex molecules into supramolecular planes parallel to *ac*. Black dashed lines represent π-π stacking interactions, red and green dashed lines represent O-H···O, C-H···O and C-H···Cl hydrogen bonding interactions, respectively. Symmetry codes: (iv) -x, 1-y, 1-z; (v) -x, -y, -z; (viii).

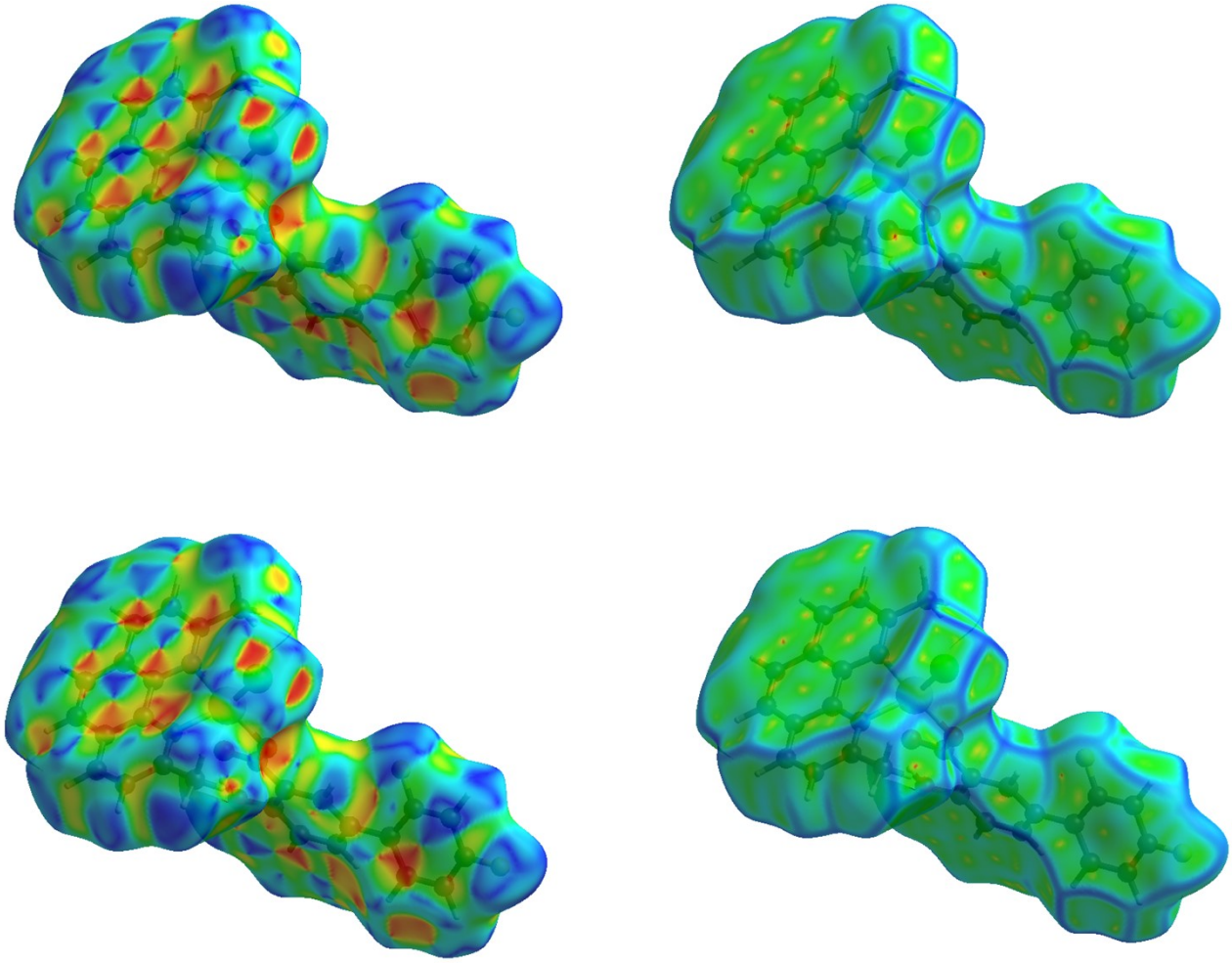

Fig. S7 Hirshfeld surface showing shape index (left) and curvedness (right) for complex **1** (top) and **2** (bottom). The surface is visualized as transparent for the sake of clarity.

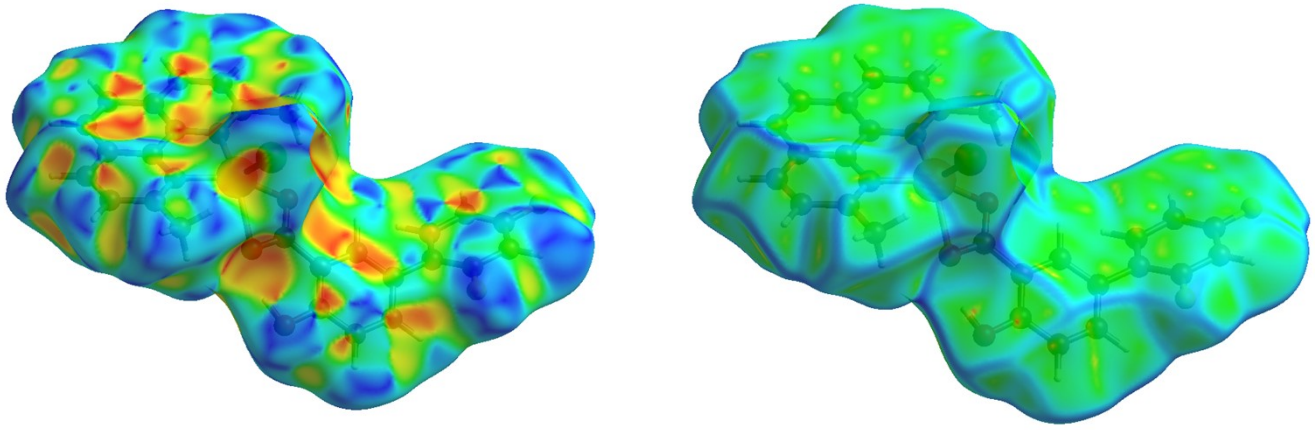

Fig. S8 Hirshfeld surface showing shape index (left) and curvedness (right) for complex **3**. The surface is visualized as transparent for the sake of clarity.

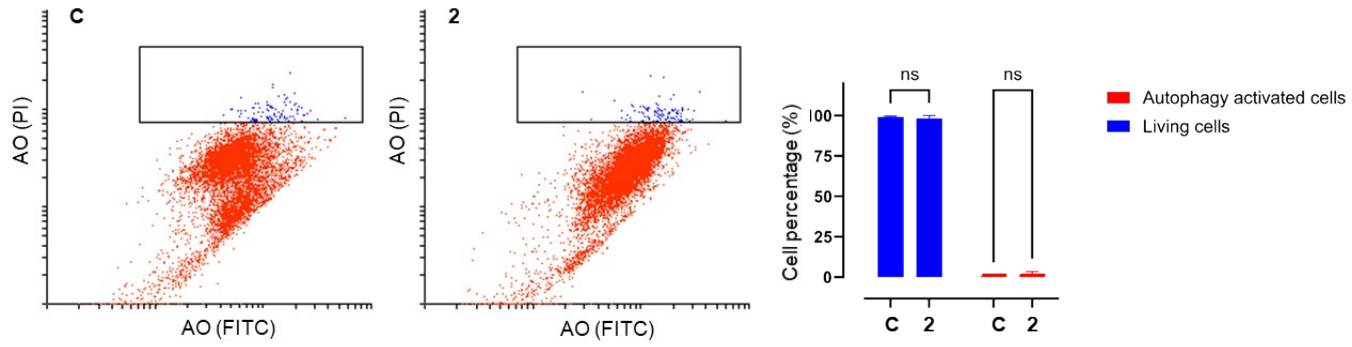

Fig. S9 Autophagic response of the PC-3 cells (48 h treatment; **C** = control, **2** = [CoCl(*dif*)(*neo*)]).

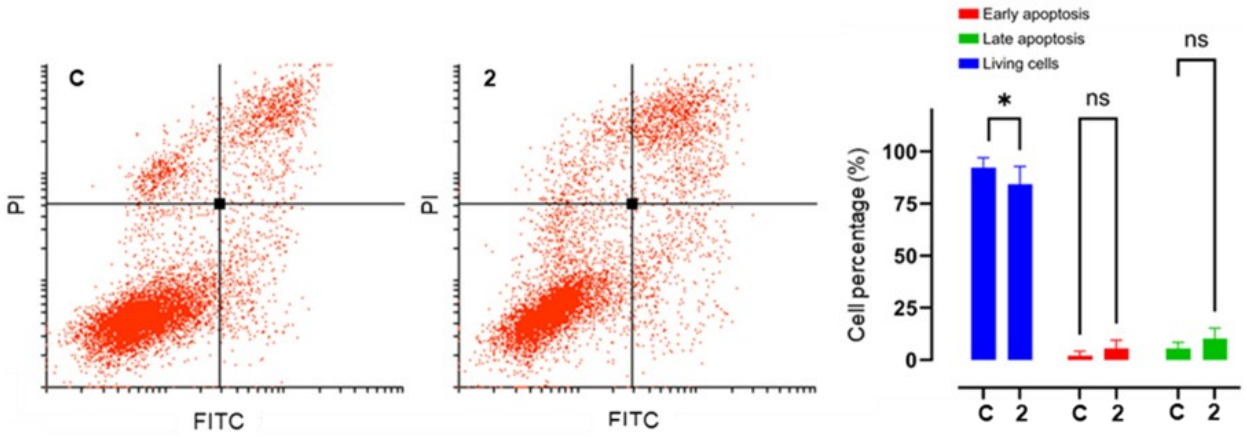

Fig. S10 Effect of **2** on induction of apoptosis in PC-3 cell line (48 h treatment; **C** = control, **2** = [CoCl(*dif*)(*neo*)]).

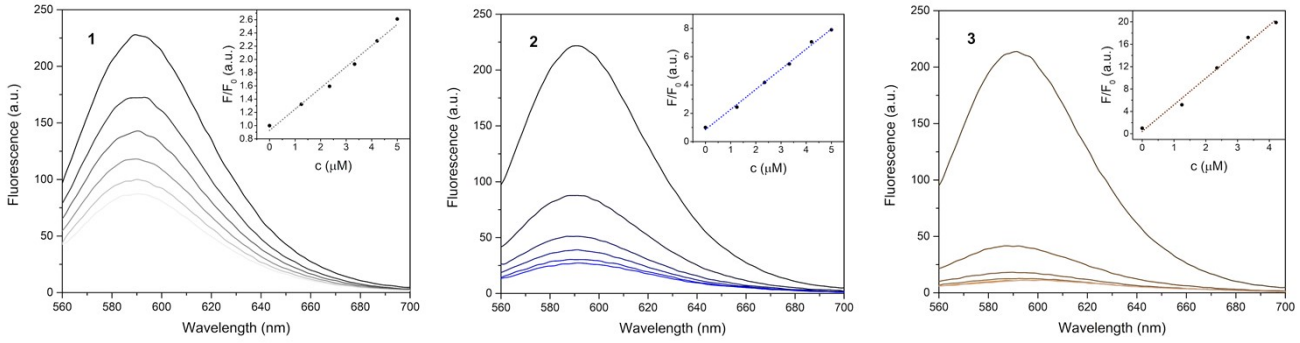

Fig. S11 Fluorescence emission spectra of DNA-EB complex (λ_{ex} = 520 nm) prepared by using isolated genomic DNA samples from studied cell lines PC3 (top), HCT116 (middle) and MDA-MB-468 (bottom) upon gradual addition of studied complexes (1 = gray, 2 = blue, 3 = brown) in the concentration range 0 – 5 μM.

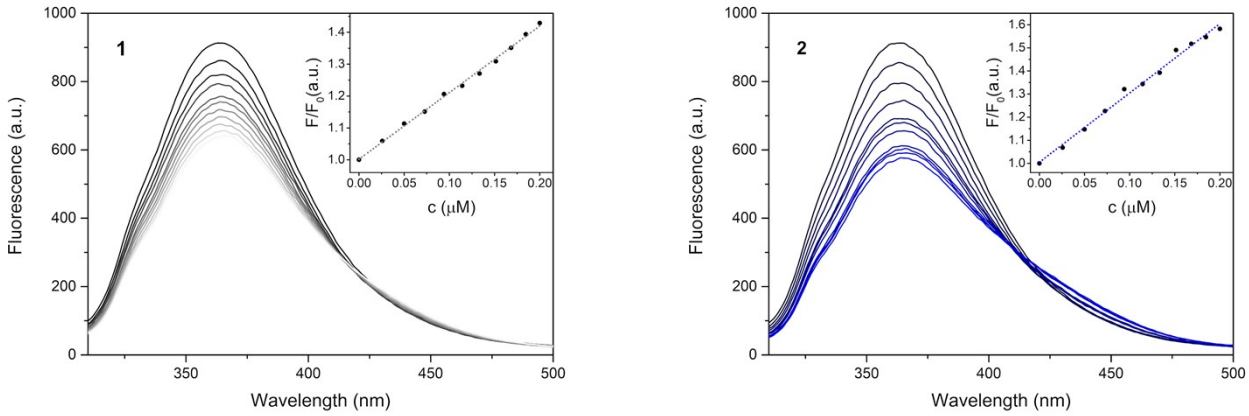

Fig. S12 Fluorescence emission spectra of HSA (λ_{ex} = 295 nm) upon addition of complexes **1** (left) and **2** (right). Insets show the linear-fitted Stern-Volmer plots.

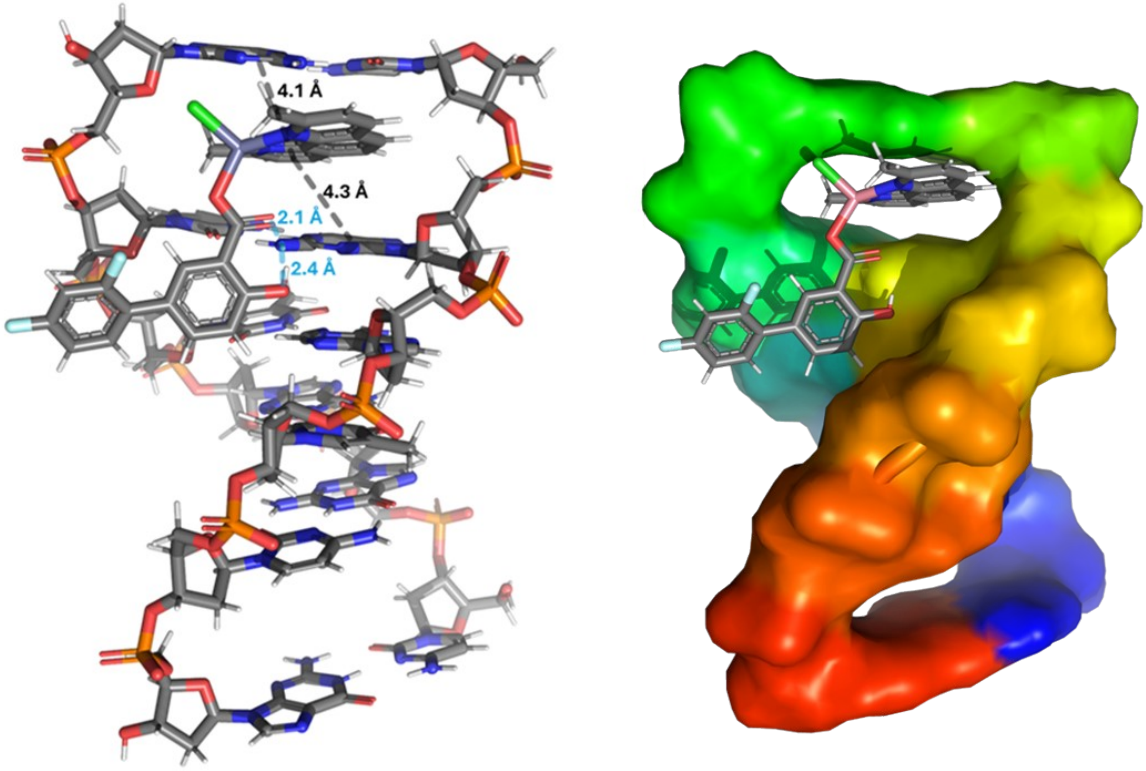

Fig. S13 Visualization of the DNA docking experiments showing complex **1** in DNA (PDB 1Z3F). The hydrogen bonds are shown as blue dashed lines and π-π stacking interactions are black. DNA surface with intercalating molecules is shown on the left.

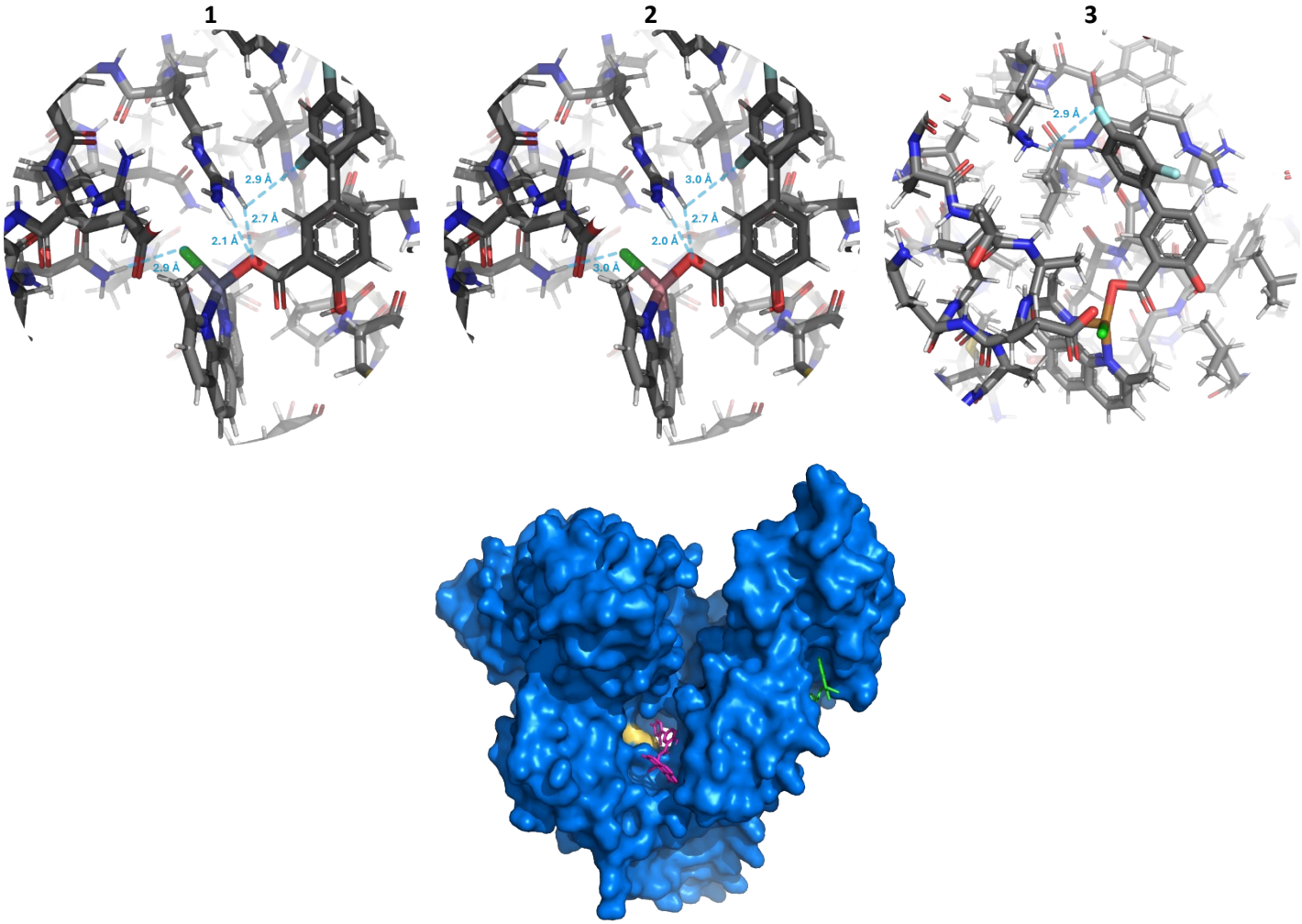

Fig. S14 Visualization of molecular docking of **1**-**3** within the structure of human serum albumin (PDB 2bxe) showing intermolecular interactions (blue dashed lines) with neighbouring amino acid residues and view of different predominant binding sites of **1** and **2** (magenta) and **3** (green), respectively. Yellow colour represents the tryptophan residue.